33RD CONGRESS
OF THE INTERNATIONAL COUNCIL
OF THE AERONAUTICAL SCIENCES
STOCKHOLM, SWEDEN, 4-9 SEPTEMBER, 2022

ICAS 2022 SWEDEN

STRUCTURAL ANALYSIS OF TWISTED/CURVED BEAMS USING A HYBRID METHOD

Ali Siami[1], Fred Nitzsche[2]

[1]Postdoctoral fellow, Carleton University, Ottawa, Canada
[2]Emeritus professor, Carleton University, Ottawa, Canada

Abstract

This paper presents a numerical approach for the structural dynamic analysis of initially twisted and curved beams. The variational asymptotical beam sectional theory due to Hodges is used to extract the set of nonlinear equations associated to the two-dimensional (2D) beam cross-sectional analysis. The conventional analytical perturbation solution is used as a first guess for the set of nonlinear equations obtained from the 2D analysis. To compensate for the effect of neglecting the higher order terms, which have been eliminated in the perturbation solution, the Firefly algorithm (FA), an iterative solution method is introduced to the problem for the first time. To reduce the sensitivity of the iterative method to the initial values, the perturbation solution provides an initial guess for the FA. The stiffness matrix obtained from the Firefly algorithm for twisted/curved beam is then further used in the geometrically exact, fully intrinsic one-dimensional beam equations to analyze its dynamic behavior. The effect of flexible joints is introduced to the equations to consider more realistic boundary conditions. The accuracy of the proposed approach is evaluated by comparing the eigenfrequencies of an initially twisted blade with the results of a three-dimensional finite-element modal analysis performed in ANSYS. Finally, the Campbell diagram of an initially twisted rotating blade is extracted using the developed method to demonstrate that it provides a fast and accurate solution to this problem.

Keywords: cross-sectional analysis, twisted/curved beam, flexible joints, firefly algorithm.

1. Introduction

The models based on three-dimensional (3D) Finite Element Analysis (FEA) possess significant precision advantages. However, one-dimensional (1D) models play a crucial role in structural analysis because they are computationally economical and provide the designer with simple tools to analyze various problems. One-dimensional beam models can be investigated using classical or refined theories in both geometrically linear and nonlinear regimes that include different levels of accuracy to evaluate the static and dynamic characteristics. These equations have been developed based on a fully intrinsic formulation. It means they do not need the displacement and rotation variables. Therefore, they are free of infinite-degree nonlinearities found in other types of formulations.

To provide the cross-sectional properties for 1D models, the Variational-Asymptotic Method (VAM) due to Hodges and colleagues has received considerable interest from researchers in the field of dynamics. VAM is computationally more efficient than 3D FEA. It starts by considering the elastic energy functional based on small parameters associated with slender beams and solve general problems involving the minimization of this functional. Berdichevskii [1] and Hodges [2] appear to be the first to split a 3D geometrically nonlinear elasticity analysis of slender structures into a nonlinear 1D analysis in the spanwise direction and a cross-sectional 2D analysis. The details about this analysis can be found in [2] to [6]. The approximate solution developed for the cross-sectional analysis is based on an analytical perturbation method. This solution for the set of nonlinear intrinsic equations is presented in [7]. As it has been shown, the perturbation solution is sensitive to the high values of initial twist and curvatures.

Many papers have been published on the geometrically exact beam theory; for example, see [8] to[12]. In [13] comprehensive review of the state-of-the art by focusing on the vibrations, dynamics and control aspects of rotating blade was provided. An energy-consistent Galerkin approach was developed by Patil and Althoff [14]. The Galerkin approach provides accurate results with fewer degrees of freedom as compared to a low-order finite-element formulation. This approach can capture the dominant nonlinearities in the system and is ideal for the use in aeroelasticity, preliminary and control design [15]. Forced vibration [16] and bifurcation analysis of rotating composite beams were also studied [17]. In [18], the intrinsic first order nonlinear equations were derived considering different connections between the hub and the blade and solved using an incremental method.

In the present work, the theoretical background of the variational asymptotic beam section analysis and a perturbation solution for the set of nonlinear equations is presented briefly. Then, an iterative numerical method is used for the 2D cross-sectional analysis to increase the accuracy of the approximated solution obtained from the perturbation method. The Galerkin approach is used to solve the 1D geometrically exact intrinsic nonlinear equations. The eigenfrequencies of an initially twisted blade are calculated using the developed codes. The results of the proposed methodology are tested against a modal analysis of the 3D FEA model of the blade performed in ANSYS. Next, the Campbell diagram of a rotating blade subjected to rigid boundary conditions is obtained as the final output of the developed structural dynamics package. Flexible joints can be also considered in the developed formulation.

2. Variational Asymptotic Beam Sectional Analysis

The papers should be prepared, if possible, using the format like this document.

The behavior of an elastic body is completely determined by its elastic energy. First, to derive 1D beam theory, the 3D energy is represented using 1D quantities. This dimensional reduction is performed by the variational asymptotic method (VAM), a powerful mathematical tool. For rotor blades, VAM splits the original nonlinear 3D formulation into a 2D cross-sectional analysis and a 1D nonlinear beam analysis for the reference line, as seen in Figure 1. More details about this method can be found in Refs. [1] to [5].

To analyze slender structures using beam theory, the VAM, and the finite element method (FEM) are combined to obtain an asymptotically correct expression for the sectional strain energy based on a discretized warping field. In the next step, the strain energy is transformed into a form compatible with the generalized Timoshenko beam theory to simplify the method. In this case, the energy expressions are used to identify the cross-section stiffness matrices of the Timoshenko formulation. To present the formulations, the 1D strain measures of classical beam theory is introduced as:

$$\bar{\epsilon} = [\bar{\gamma}_{11} \quad \bar{\kappa}_1 \quad \bar{\kappa}_2 \quad \bar{\kappa}_3]^T \tag{1}$$

where $\bar{\gamma}_{11}$ is the extensional strain measure, $\bar{\kappa}_1$ is the torsional strain measure, and $\bar{\kappa}_\alpha$ (for $\alpha = 2, 3$) are bending strain measures. The 2nd-order asymptotically correct sectional energy in explicit form can be obtained (see [6] and [7]) as:

$$2U = \bar{\epsilon}^T A\bar{\epsilon} + 2\bar{\epsilon}^T B\bar{\epsilon}' + \bar{\epsilon}'^T C\bar{\epsilon}' + 2\bar{\epsilon}^T D\bar{\epsilon}'' \tag{2}$$

The coefficient matrices are presented the above equation ($A, B, C\ and\ D$) can be found in Ref. [6].

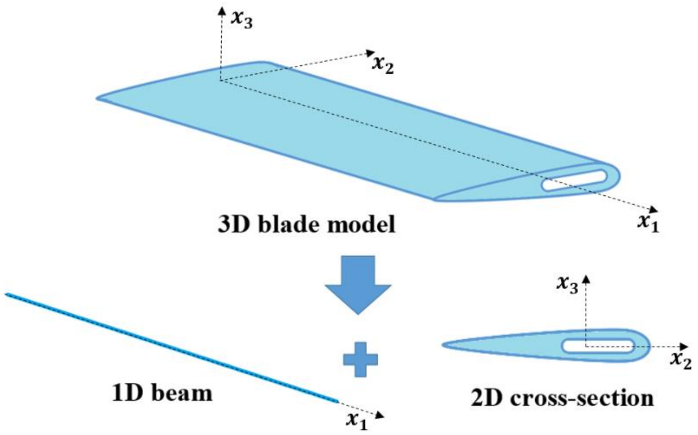

Figure 1 – The decomposition of a three-dimensional blade to the 2D and 1D models.

The generalized Timoshenko theory is the most common beam model for the variational asymptotical beam sectional analysis. The sectional strain energy in the generalized Timoshenko theory is given by [6]:

$$2U = \epsilon^T X \epsilon + 2\epsilon^T Y \gamma_s + \gamma_s^T G \gamma_s \tag{3}$$

where X, Y and G are the different submatrices of the stiffness matrix, which can be written as:

$$K_T = \begin{bmatrix} X & Y \\ Y^T & G \end{bmatrix} \tag{4}$$

In addition, the 1D-strain measures in a generalized Timoshenko model are defined as follows:

$$\epsilon = [\gamma_{11} \quad \kappa_1 \quad \kappa_2 \quad \kappa_3]^T \ , \gamma_s = [2\gamma_{12} \quad 2\gamma_{13}]^T \tag{5}$$

where $2\gamma_{12}$ and $2\gamma_{13}$ represent rotations of the cross-section about the x_3 and x_2 axes, respectively. In addition, γ_{11} is the extensional strain measure, $\kappa_1$is the torsional strain measure, and κ_α (for $\alpha = 2,3$) are bending strain measures in the Timoshenko model presentation of the sectional strain energy. To accomplish the desired kinematics, the 1D constitutive law and the 1D static equilibrium equations are combined in the next steps. It has been shown in [5] that the kinematic relationships between the strain measures assuming small values of γ_{12} and γ_{13} can be written as:

$$\bar{\gamma}_{11} = \gamma_{11} \quad , \quad \bar{\epsilon} = \epsilon + Q\gamma_s' + P\gamma_s \tag{6}$$

where

$$Q = \begin{bmatrix} 0 & 0 \\ 0 & 0 \\ 0 & -1 \\ 1 & 0 \end{bmatrix} \quad , \quad P = \begin{bmatrix} 0 & 0 \\ k_2 & k_3 \\ -k_1 & 0 \\ 0 & -k_1 \end{bmatrix} \tag{7}$$

It should be noted that k_1 in the above equation is the initial twist and k_α ($\alpha = 2,3$) are the initial curvature components of the reference line about x_α.

Now, the target is to find expression for matrices X, Y and G by using the presented equations. To obtain the Timoshenko-like stiffness matrix, the following relations can be written by equating Eq. (2) and Eq. (3) (see Ref. [9]):

$$\begin{gathered} X = X_A + X_B + X_C + X_D \\ Y = Y_A + Y_B + Y_C + Y_D \\ G = G_A + G_B + G_C + G_D \end{gathered} \tag{8}$$

where the subscript indicates the matrix source of the contribution. For example, Y_A indicates the contribution to Y from the stiffness matrix A. These individual contributions are presented in Appendix. Based on the presented equations, the problem becomes finding X, Y and G that satisfies Eq. (8). The resulting system of equations are a set of nonlinear equations in X, Y and G. In this work, these equations are solved using an analytical perturbation and a numerical iterative method.

3. The solution methods for the 2D cross-sectional analysis

3.1 Perturbation solution

The generalized Timoshenko stiffness presented by Eq. (8) can be obtained using perturbation methods with accuracy up to second order with respect to k_i $(i = 1, 2, 3)$. The detail of this solution for the cross-sectional analysis are found in [7]. The solution of the nonlinear equations presented in Eq. (8) up to the zeroth order with respect to k_i is shown in Eq. (9). The corresponding first and second-order solutions can be found in [7].

$$\begin{gathered} G_0 = [Q^T A^{-1}(C - B^T A^{-1} B) A^{-1} Q]^{-1} \\ Y_0 = B^T A^{-1} Q G_0 \\ X_0 = A + Y_0 G_0^{-1} Y_0^T \end{gathered} \tag{9}$$

3.2 Numerical solution algorithm

The firefly algorithm (FA) was introduced based on the behavior of fireflies and their flashing pattern to attract each other. The algorithm can be summarized in the following three steps [21]:

1) A firefly can attract other fireflies without considering their sex: fireflies are unisex.
2) For each two flashing fireflies, the brighter one will attract the less bright towards itself. If there is no brighter than a particular firefly, it will move randomly.
3) The brightness of a firefly is determined by the objective function.

It should be noticed that the attractiveness of each firefly is directly proportional to its light intensity. The variation of attractiveness, β^f can be defined as:

$$\beta^f = \beta_0^f e^{-\gamma^f r^2} \tag{10}$$

where r is the distance between two adjacent fireflies, β_0^f is the attractiveness at $r = 0$, and γ^f is a constant named light absorption coefficient that controls the speed of the FA convergence. The movement of a firefly i towards position of a brighter (higher attractive) one is determined as follows:

$$Xf_i^{k+1} = Xf_i^k + \beta_0^f \, e^{-\gamma^f r_{ij}^2}\left(Xf_j^k - Xf_i^k\right) + \alpha_k \epsilon_i^k \tag{11}$$

where α_k is randomization parameter and ϵ_i^k is a vector of random number drawn from Gaussian distribution at the time step k, and $r_{ij}$is distance between fireflies i and j. In each loop, the distances of each pair of fireflies are updated. For applying the algorithm, the population of fireflies N_G and number of iterations N_I should be first specified. It should be noted that α_k controls the diversity of solutions and it can vary with the iteration counter k. Generally, for most applications, it is chosen as $\alpha_k \in [0,1]$. Introducing L^f as the average scale of the problem of interest, γ^f can be made $1/\sqrt{L^f}$. However, it should be considered that the cost of the FA computation is $O(N_G^2 N_I)$. Therefore, the use of larger numbers of generations in order to improve the results of the algorithm is limited [21].

3.3 Hybrid solution algorithm

In this work, the hybrid solution is introduced to solve the set of nonlinear equations presented in Eq. (8). First, the perturbation solution up to the second order with respect to small parameters related to the beam initial twist/curvatures is used to solve the Timoshenko stiffness equations. Then, this perturbation solution is considered as an initial guess for the iterative method. Therefore, the initial fireflies' generation is defined based on the perturbation solution in order to limit the searching domain of the iterative solution to a narrow region around the perturbation solution. It was observed that the present hybrid method allows for keeping the positive aspects of both the perturbation and iterative methods as the main problem related to the iterative method is its sensitivity to the initial guess. This issue is here eliminated by using the solution of perturbation method as the initial value for the iterative one. Most importantly, by using the firefly algorithm for solving the set of nonlinear equations presented in Eq. (8), the results of the perturbation solution can be improved.

For the iterative method, the following rearrangement of Eq. (8) is introduced:

$$\begin{gathered} F_X = X_A + X_B + X_C + X_D - X = 0 \\ F_Y = Y_A + Y_B + Y_C + Y_D - Y = 0 \end{gathered} \tag{12}$$

$$F_Y = G_A + G_B + G_C + G_D - G = 0$$

Using Eq. (12), the target function (in vector form) of the Firefly algorithm is defined as:

$$F_{min}^{vec} = [F_X^{vec}, F_Y^{vec}, F_G^{vec}]^T \tag{13}$$

where

$$\begin{aligned} F_X^{vec} &= [F_X(1,1{:}4), F_X(2,2{:}4), F_X(3,3{:}4), F_X(4,4{:}4)]^T \\ F_Y^{vec} &= [F_Y(1,1{:}2), F_Y(2,1{:}2), F_Y(3,1{:}2), F_Y(4,1{:}2)]^T \\ F_G^{vec} &= [F_G(1,1{:}2), F_G(2,2{:}2)]^T \end{aligned} \tag{14}$$

where in the above equations the first index inside the parentheses specifies the row of the matrix and the second and third indices show the starting and ending columns inside of the corresponding matrix. For example, $F_X(1,1{:}4)$ represents the first raw of matrix F_X. Based on Eqs. (13) and (14), the target function for the minimization problem becomes a vector with 21 elements after considering the symmetry of the submatrices X and G in the stiffness matrix presented in Eq. (4).

4. One- dimensional intrinsic beam equations

The intrinsic equations governing the dynamics of a general, non-uniform, twisted, curved, anisotropic beam undergoing large deformation are given as follows (see [20])[1]:

$$F' + (\tilde{k} + \tilde{K})F + f_{ext} = \dot{P} + \tilde{\Omega}P \tag{15}$$

$$M' + (\tilde{k} + \tilde{K})M + (\tilde{e}_1 + \tilde{\Gamma})F + m_{ext} = \dot{H} + \tilde{\Omega}H + \tilde{V}P \tag{16}$$

$$V' + (\tilde{k} + \tilde{K})V + (\tilde{e}_1 + \tilde{\Gamma})\Omega = \dot{\Gamma} \tag{17}$$

$$\Omega' + (\tilde{k} + \tilde{K})\Omega = \dot{K} \tag{18}$$

where $(\,)'$ denotes the derivative with respect to the beam reference line and $\dot{(\,)}$ is the absolute time derivative. $F(x,t)$ and $M(x,t)$ denote the inertial force and moment vector, $P(x,t)$ and $H(x,t)$ are the linear and angular momentum vectors, $\Gamma(x,t)$ and $K(x,t)$ are the beam strain and local curvatures. In addition, $V(x,t)$ and $\Omega(x,t)$ are the linear and angular velocities. The external force and moment caused by aerodynamic effects, for example, are denoted by $f_{ext}(x,t)$ and $m_{ext}(x,t)$, respectively. The initial curvature and twist of the beam are grouped in the vector $k = [k_1 \quad k_2 \quad k_3]^T$ and $e_1 = [1 \quad 0 \quad 0]^T$ is the unit vector in the axial direction, x_1 according to Figure 1. It should be noted that the tilde transforms the vector cross operation $y\times$ into its matrix multiplication equivalent, $\tilde{y}$.

The intrinsic beam equations provide four vector equations for eight vector unknowns, $(F, M, P, H, \Gamma, K, V, \Omega)$. Therefore, four more vector equations are needed. Two equations relate the generalized forces (F, M) and the generalized strains (Γ, K) via the beam cross-section stiffness matrix. The relationships between the generalized momenta (P, H) and the generalized velocities (V, Ω) can be built using the beam cross-section inertia matrix. These additional equations are (see [2] and [3]):

$$\begin{Bmatrix} F \\ M \end{Bmatrix} = \begin{bmatrix} \mathbb{U} & \mathbb{V} \\ \mathbb{V}^T & \mathbb{W} \end{bmatrix} \begin{Bmatrix} \Gamma \\ K \end{Bmatrix} \tag{19}$$

$$\begin{Bmatrix} P \\ H \end{Bmatrix} = \begin{bmatrix} \mathbb{G} & \mathbb{K} \\ \mathbb{K}^T & \mathbb{I} \end{bmatrix} \begin{Bmatrix} V \\ \Omega \end{Bmatrix} \tag{20}$$

where $\mathbb{U}$, $\mathbb{V}$ and $\mathbb{W}$ are the stiffness submatrices obtained from the cross-sectional analysis. The inertia-related matrices take the form:

$$\begin{gathered} \mathbb{G} = \mu I = \begin{bmatrix} \mu & 0 & 0 \\ 0 & \mu & 0 \\ 0 & 0 & \mu \end{bmatrix}, \qquad \mathbb{K} = \begin{bmatrix} 0 & \mu\bar{\xi}_3 & -\mu\bar{\xi}_2 \\ -\mu\bar{\xi}_3 & 0 & 0 \\ \mu\bar{\xi}_2 & 0 & 0 \end{bmatrix}, \\ \mathbb{I} = \begin{bmatrix} \mathbb{i}_2 + \mathbb{i}_3 & 0 & 0 \\ 0 & \mathbb{i}_2 & \mathbb{i}_{23} \\ 0 & \mathbb{i}_{23} & \mathbb{i}_3 \end{bmatrix} \end{gathered} \tag{21}$$

where μ, $\bar{\xi}_2$, $\bar{\xi}_3$ and $\mathbb{i}_2$, $\mathbb{i}_3$ and $\mathbb{i}_{23}$ are the mass per unit length, offsets from the reference line of the cross-sectional mass centroid, and the two cross-sectional mass momenta and the product of inertia per unit length, respectively. These values are calculated in the cross-sectional analysis.

To solve Eqs. (15) to (20), a variable order finite element method is used (see [20]). The blade is discretized into n elements along the span as shown in Figure 2. The shifted Legendre polynomials are used here as the independent trial functions. Assuming uniform structural properties along each element, the discretized equations can be obtained from Eq. (15) to (20). The details and the derivations can be found in [20], where the 1D beam nonlinear equation is demonstrated to assume the following form:

$$A_{kj}\dot{q}_j(t) + B_{kj}q_j(t) + C_{kjr}q_j(t)q_r(t) + D_k + F_k^{ext}(t) + M_k^{ext}(t) = 0 \tag{22}$$

where $i, j \; and \; k = 1,2, \dots m$ and m indicates the number of modes used in the variable order finite element method. Considering n as the number of elements for the discretization, the total variable vector is $q(t) = [q^1(t), q^2(t), \dots, q^n(t)]^T$, and $q^i(t)$ is the time dependent component of the unknown variables at each element:

$$q^i(t) = \left[v_1^i(t), \omega_1^i(t), \gamma_1^i(t), \kappa_1^i(t), \dots, v_m^i(t), \omega_m^i(t), \gamma_m^i(t), \kappa_m^i(t) \right]^T \tag{23}$$

where v, ω, γ and κ represent the time variable parts of velocity (V), angular velocity (Ω), strain (Γ) and curvature (K), respectively. These variables have been introduced to the problem after the separation of variables in time and space domains (see Ref. [20]). In addition, $F_k^{ext}(t)$ and $M_k^{ext}(t)$ are the terms related to external loads that appear in the equations if external distributed loads are applied to the elements. It should be noted that the coefficients matrices (A_{kj}, B_{kj}, C_{kjr} and D_k) appeared in Eq. (22) can be found in Ref. [20].

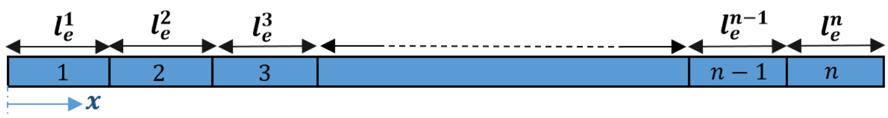

Figure 2 – A blade divided to n-element along the span [20].

For the subsequent modal analysis, the system of equations needs to be linearized around a steady-state solution. The steady-state solution of Eq. (22) can be determined by solving the following equations:

$$B_{ki}q_i^0 + C_{kij}q_i^0 q_j^0 + \bar{D}_k = 0 \tag{24}$$

where q^0 refers to the desired steady-state solution due to the steady-state forcing provided in $\bar{D}$. The solution is found using Newton-Raphson iterations, where the required Jacobian is obtained taking the derivatives of Eq. (24) with respect to q^0:

$$\mathcal{J}(q) = B_{ki} + C_{kji}q_i^0 + C_{kij}q_j^0 \tag{25}$$

To formulate the eigenvalue problem, the 1D beam equations seen in Eq. (22) are next linearized. The general solution of the nonlinear system of equations is represented as:

$$q(t) = q^0 + q^*(t) \tag{26}$$

where $q^*(t)$ is a small perturbation about the steady-state solution. After linearization, the natural frequencies and corresponding mode shapes can be calculated from:

$$\hat{A}_{ki}\dot{q}_i^* + \hat{B}_{ki}q_i^* = 0 \tag{27}$$

where

$$\hat{A}_{ki} = A_{ki} \;\; , \;\; \hat{B}_{ki} = B_{ki} + \left(C_{kij} + C_{kji}\right)q_j^0 \tag{28}$$

5. Results

In this part, the results from the asymptotically correct cross-sectional analysis code developed in MATLAB are presented. The developed code can take different type of grids and their combinations, including triangular (linear and quadratic) and quadrilateral elements (linear and quadratic) as input. In addition, the developed package can deal with anisotropic materials.

In this work, the results of the package for a blade with initial twist ($k_1 = 0.6283 \, rad/m$) and a NACA0012 airfoil cross section is presented. The geometrical and material properties of this blade are given in Table 1. The cross section of the blade generated using quadrilateral elements is plotted in Figure 3. In Table 2, selected elements of the obtained stiffness matrix are tabulated. The values presented in the first row of Table 2 correspond to the Euclidian norm of the target function given by Eq. (13) divided by the norm of the vector defined by the 21 elements of the stiffness matrix obtained from the perturbation solution, to give an indication of the convergence of the proposed method. For the Firefly algorithm results presented in Table 2 the values $N_G = 100$ and $N_I = 100$ were taken. It can be seen from these values that the hybrid method (analytical perturbation combined with the numerical Firefly Algorithm) minimizes the target function better that the corresponding results obtained with the perturbation solution alone. This is an indication that the proposed hybrid method increases the accuracy of the solution considerably.

Table 1 – Properties of initially twisted blade.

Geometrical properties	
Airfoil	NACA0012
Chord length	0.135 $[m]$
Length of blade	2 $[m]$
Initial twist	0.6283 $[rad/m]$
Material properties	
Young's Modulus (E)	7.1×10^{10} $[Pa]$
Shear Modulus (G)	2.6692×10^{10} $[Pa]$
Poisson's ratio (ν)	2770 $[kg/m^3]$
Density (ρ)	0.33

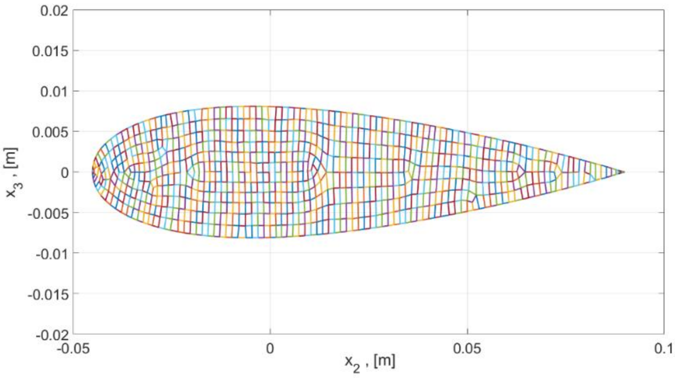

Figure 3 – The cross-section of airfoil (NACA0012) with quadrilateral elements

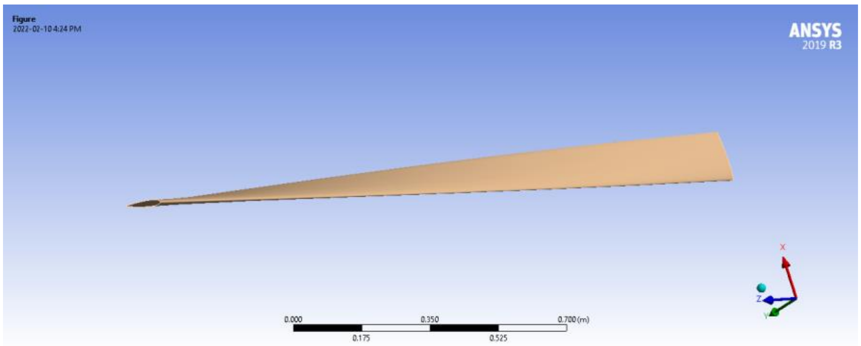

Figure 4 – Blade with initial twist.

To further compare the accuracy of the calculated cross-sectional properties (i.e., from the stiffness and mass matrices), the eigenfrequencies of the blade with clamped-free boundary conditions are compared with the corresponding results of a modal analysis performed in ANSYS. These results are obtained for a twisted blade with $2\ m$ length. The eigenfrequencies of the blade are calculated solving the eigenvalue problem presented in Eq. (27). Table 3 shows the fifteen first eigen-frequencies of the blade using the stiffness matrices calculated from the perturbation solution alone and the Firefly

Algorithm hybrid method, respectively. The table shows that the calculated frequencies are very similar to the ones obtained from the modal analysis with the complete FEA 3D model in ANSYS. It should be noted that for the cross-sectional analysis of the blade 1167 nodes have been used and for the 1D model of the blade only 21 nodes along the span of blade were utilized. It was observed that this number of nodes provides results that they are no longer sensitive to the discretization.

Table 2 – Stiffness of the blade (NACA0012 airfoil) with initial twist ($k_1 = 0.6283\ rad/m$).

Target function and stiffness values	**Cross-sectional analysis (perturbation solution alone)**	**Cross-sectional analysis (hybrid method)**
$\lVert F_{min}\rVert/\lVert K_p^{vec}\rVert$	0.0113	0.0035
X_{11}, $[N]$	1.0562×10^8	1.0545×10^8
X_{22}, $[N.m^2]$	2.6970×10^3	2.6870×10^3
X_{33}, $[N.m^2]$	1.6029×10^3	1.596×10^3
X_{44}, $[N.m^2]$	1.1851×10^5	1.1815×10^5
X_{21}, $[N.m]$	7.6240×10^4	7.305×10^4
X_{41}, $[N.m]$	-1.1898×10^6	-1.1955×10^6
G_{11}, $[N]$	3.4401×10^7	3.4690×10^7
G_{22}, $[N]$	1.1212×10^7	1.0493×10^7
Y_{12}, $[N]$	-2.5679×10^4	-1.8747×10^4
Y_{22}, $[N.m]$	4.6588×10^4	3.0633×10^4
Y_{31}, $[N.m]$	1.7512×10^3	1.06748×10^3

Based on the presented formulation, the developed package can provide the Campbell diagrams for different types of boundary conditions, including fix or flexible joints at the ends of the blade. In Figure 5, the Campbell diagram for the ten first modes the initially twisted blade within the specified rotational speed range is presented.

Table 3 – Comparing the eigenfrequencies for the blade (NACA0012 airfoil) with initial twist ($k_1 = 0.6283\ rad/m$).

Mode number	**Eigenfrequency (Hz)**		
	Stiffness matrix obtained with the perturbation solution alone	**Stiffness matrix obtained with the proposed hybrid method**	**ANSYS modal analysis with a full 3D FEA model**
1	2.807	2.799	2.805
2	10.512	10.478	10.507
3	34.516	34.377	34.411
4	44.196	44.0325	44.167
5	88.334	88.0479	88.317
6	95.291	96.805	96.892
7	141.838	141.293	141.70
8	171.494	170.746	171.26
9	225.886	225.058	225.98
10	285.883	290.398	290.64
11	316.717	315.502	316.98
12	397.158	395.375	397.21
13	430.489	428.694	430.10

14	477.5149	484.9013	484.95
15	545.157	542.638	543.04

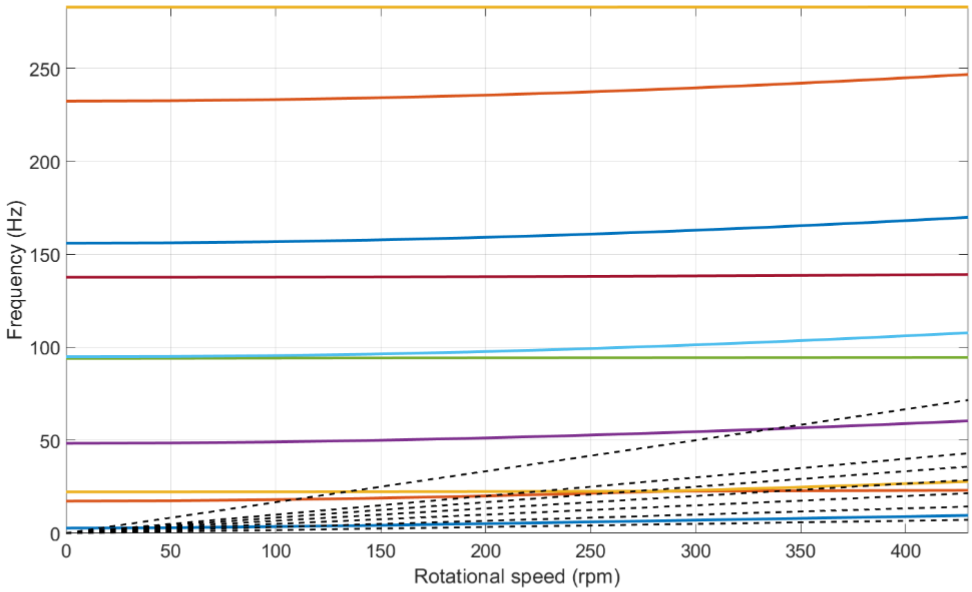

Figure 5 – Campbell diagram for the blade with rigid connections at the hub (solid lines are the calculated eigenfrequencies, black dashed lines are the harmonics of the nominal rotational speed).

6. Conclusion

The results of a complete package for the structural dynamic analysis of initially twisted/curved slender beams based on the variational asymptotic beam sectional analysis using a new approach have been presented. The approach introduces a novel hybrid strategy for the solution of the set of nonlinear equations to obtain the cross-sectional Timoshenko stiffness matrix. It is seen that the proposed approach can improve the results of the sectional analysis of the beam in the presence of relatively large initial twist and curvatures. The package includes both the 2D cross-sectional and the 1D nonlinear beam analyses. Therefore, it can be used as a self-contained computational tool for evaluation of the dynamic behavior of twisted and curved rotating blades having anisotropic material properties. The results of the hybrid approach for the cross-sectional analysis were presented for an initially twisted blade. The accuracy of the cross-sectional matrices was evaluated by comparing the eigenfrequencies calculated using the linearized 1D equations with the results of a full 3D FEA model done in ANSYS. In addition, the new package can evaluate the effect of flexible end joints in the beam dynamic analysis, which is useful for many applications, such as wind turbines having complex blade supports.

7. Contact Author Email Address

mailto: alisiami@cunet.carleton.ca

8. Copyright Statement

References

[1] Berdichevskii V L. On the energy of an elastic rod. *J. Appl. Math. Mech*, Vol. 45, pp 518-529,1981.

[2] Hodges D H. A mixed variational formulation based on exact intrinsic equations for dynamics of moving beams. *International Journal of Solids and Structures*, Vol. 26, pp 1253-1273,1990.

[3] Cesnik C E S and Hodges D H. VABS: a new concept for composite Rotor blade cross-sectional Modeling. *Journal of the American Helicopter Society*, Vol. 42, No. 1, pp 27-38,1997.

[4] Hodges D H. Geometrically exact, intrinsic theory for dynamics of curved and twisted anisotropic beams. *AIAA Journal*, Vol. 41, No. 6, pp 1131-113, 2003.

[5] Yu W, Hodges D H, Volovoi V and Cesnik C E S. On Timoshenko-like modeling of initially curved and twisted composite beams. *International Journal of Solids and Structures*, Vol. 39. pp 5101-5121,2002.

[6] Hodges D H. *Nonlinear composite beam theory*. AIAA ,2006.

[7] Yu W, Hodges D H and Ho J C. Variational asymptotic beam sectional analysis – An updated version. *International Journal of Engineering Science*, Vol. 59, pp 40-64, 2012.

[8] Hodges D H, Atılgan A R, Fulton M V and Rehfield L W. Free-vibration analysis of composite beams. *Journal of the American Helicopter Society*, Vol. 36, No. 3, pp 36-47,1991.

[9] Ho J, Yu W and Hodges D H. Energy transformation to generalized Timoshenko form by the variational asymptotic beam sectional analysis. *51st AIAA/ASME/ASCE/AHS/ASC Structures, Structural Dynamics, and Materials Conference*, Orlando, Florida, 2010.

[10] Shang X, Hodges D H, and Peters D A. Aeroelastic stability of composite hingeless rotors in hover with finite-state unsteady aerodynamics. *Journal of the American Helicopter Society*, Vol. 44, No. 3, pp 206 – 221,1999.

[11] Ghorashi M and Nitzsche F. Comparison of the variational asymptotic beam sectional analysis methods applied to composite beams. *Proceedings of the 18th International Conference of Adaptive Structures and Technologies*, Ottawa, Canada, 2007.

[12] Ghorashi M and Nitzsche F. Steady state nonlinear dynamic response of a composite rotor blade using implicit integration of intrinsic equations of a beam. *International Review of Aerospace Engineering*, Vol. 1, pp 225-233, 2008.

[13] Ghorashi M and Nitzsche F. Nonlinear dynamic response of an accelerating composite rotor blade using perturbations. *Journal of Mechanics of Materials and Structures*, Vol. 4, No. 4, pp 693 –718, 2009.

[14] Patil M J and Althoff M. Energy-consistent, Galerkin approach for the nonlinear dynamics of beams using intrinsic equations. *Journal of Vibration and Control*. Vol. 17, pp 1748-1758, 2011.

[15] Althoff M, Patil M J and Traugott J P. Nonlinear modeling and control design of active Helicopter blades. *Journal of the American Helicopter Society*, Vol. 57, pp 1-18, 2012.

[16] Bekhoucha F, Rechak S, Duigou L and Cadou J. Nonlinear forced vibrations of rotating anisotropic beams. *Nonlinear Dynamics*, Vol 74, pp 1281-1296, 2013.

[17] Bekhoucha F, Rechak S, Duigou L and Cadou J. Branch switching at Hopf bifurcation analysis via asymptotic numerical method: application to nonlinear free vibrations of rotating beams. *Communications in Nonlinear Science and Numerical Simulation*, Vol. 22, pp 716-730, 2015.

[18] Sotoudeh Z and Hodges D H. Structural dynamics analysis of rotating blades using fully intrinsic equations, part I: formulation and verification of single-load-path configurations. *Journal of the American Helicopter Society*, Vol. 58, No. 3, pp 1-9, 2013.

[19] Patil M J and Hodges D H. Variable-order finite element for nonlinear, fully intrinsic beam equations. *Journal of Mechanics of Materials and Structures*, Vol. 6. No. 1-4, pp 479-493, 2011.

[20] Siami A, Nitzsche F, Leibbrandt R, Spieß C and Hilewit D. Dynamic response analysis of the helicopter blades with non-uniform structural properties. *AIAA Scitech Forum*, Virtual event, 0562, 2021.

[21] Siami A, Karimi H R, Cigada A, Zappa E and Sabbioni E. Parameter optimization of an inerter-based isolator for passive vibration control of Michelangelo's Rondanini Pietà. *Mechanical Systems and Signal Processing*, Vol. 98, pp 667–683, 2018.

Appendix: The stiffness matrix of the Timoshenko uniform beam model

The individual contributions of different terms in Eq. (8) can be presented as follows (see Ref. [9])

$$
\begin{aligned}
X_A &= (\Delta_{4\times4} - Q[Z]_{21})^T A(\Delta_{4\times4} - Q[Z]_{21}) \\
X_B &= 2(\Delta_{4\times4} - Q[Z]_{21})^T B(Q[Z_2]_{21} - [Z]_{11} - P[Z]_{21}) \\
X_C &= (Q[Z_2]_{21} - [Z]_{11} - P[Z]_{21})^T C(Q[Z_2]_{21} - [Z]_{11} - P[Z]_{21}) \\
X_D &= 2(\Delta_{4\times4} - Q[Z]_{21})^T D([Z_2]_{11} - Q[Z_3]_{21} + P[Z_2]_{21})
\end{aligned} \tag{29}
$$

$$
\begin{aligned}
Y_A &= (\Delta_{4\times4} - Q[Z]_{21})^T A(P - Q[Z]_{22}) \\
Y_B &= (\Delta_{4\times4} - Q[Z]_{21})^T B(Q[Z_2]_{22} - [Z]_{12} - P[Z]_{22}) \\
&\quad + \quad ([Z]_{11} - Q[Z_2]_{21} + P[Z]_{21})^T B^T (Q[Z]_{22} - P) \\
Y_C &= (Q[Z_2]_{21} - [Z]_{11} - P[Z]_{21})^T C(Q[Z_2]_{22} - [Z]_{12} - P[Z]_{22}) \\
Y_D &= (\Delta_{4\times4} - Q[Z]_{21})^T D([Z_2]_{12} - Q[Z_3]_{22} + P[Z_2]_{22}) \\
&\quad + \quad (Q[Z_3]_{21} - [Z_2]_{11} - P[Z_2]_{21})^T D^T (Q[Z]_{22} - P)
\end{aligned} \tag{30}
$$

and

$$
\begin{aligned}
G_A &= (P - Q[Z]_{22})^T A(P - Q[Z]_{22}) \\
G_B &= 2(P - Q[Z]_{22})^T B(Q[Z_2]_{22} - [Z]_{12} - P[Z]_{22}) \\
G_C &= (Q[Z_2]_{22} - [Z]_{12} - P[Z]_{22})^T C(Q[Z_2]_{22} - [Z]_{12} - P[Z]_{22}) \\
G_D &= 2(P - Q[Z]_{22})^T D([Z_2]_{12} - Q[Z_3]_{22} + P[Z_2]_{22})
\end{aligned} \tag{31}
$$

where $\Delta_{4\times4}$ indicates the identity matrix of dimension four, and the matrices presented by P and Q are given in Eq. (7). In addition, A, B, C and D are the coefficient matrices of the 2nd-order asymptotically correct sectional energy presented by Eq. (2) and they can be found in Ref. [6]. The matrices are partitioned such that subscript 11 refers to the partition occupying rows 1 to 4 and columns 1 to 4, subscript 12 refers to the partition occupying rows 1 to 4 and columns 5 to 6. This notation is extended to the other subscripts. It means subscript 21 points to the partition placing at rows 5 to 6 and columns 1 to 4 and subscript 22 indicates the partition occupying rows 5 to 6 and columns 5 to 6, respectively. As such, these partitions produce the following result.

$$
[Z] = \begin{bmatrix} [Z]_{11} & [Z]_{12} \\ [Z]_{21} & [Z]_{22} \end{bmatrix} \;,\; [Z_2] = \begin{bmatrix} [Z_2]_{11} & [Z_2]_{12} \\ [Z_2]_{21} & [Z_2]_{22} \end{bmatrix} \;,\; [Z_3] = \begin{bmatrix} [Z_3]_{11} & [Z_3]_{12} \\ [Z_3]_{21} & [Z_3]_{22} \end{bmatrix} \tag{32}
$$

Explicit expressions for matrices $[Z]$, $[Z]'$ and $[Z]''$ can be written as:

$$
\begin{aligned}
[Z] &= \begin{bmatrix} \bar{R} & \bar{S} \\ \bar{S}^T & \bar{T} \end{bmatrix} \left(\begin{bmatrix} D_3 & D_4 \\ D_2 & D_1 \end{bmatrix} \begin{bmatrix} X & Y \\ Y^T & G \end{bmatrix} \right) \\
[Z]' &= [Z]^2 \\
[Z]'' &= [Z]^3
\end{aligned} \tag{33}
$$

where

$$
D_1 = \begin{bmatrix} 0 & -k_1 \\ k_1 & 0 \end{bmatrix} \;,\; D_2 = \begin{bmatrix} k_3 & 0 & 0 & 0 \\ -k_2 & 0 & 0 & 0 \end{bmatrix} \;,\; D_3 = \begin{bmatrix} 0 & 0 & 0 & 0 \\ 0 & 0 & -k_3 & k_2 \\ 0 & k_3 & 0 & -k_1 \\ 0 & -k_2 & k_1 & 0 \end{bmatrix} \text{ and } \tag{34}
$$

$$
D_4 = Q - D_2^T
$$